Websites:
http://www.sciencepub.net/nature
http://www.sciencepub.net

Emails:
naturesciencej@gmail.com
editor@sciencepub.net

Nature and Science

MARSLAND PRESS
Multidisciplinary Academic Journal Publisher

Detection Efficiency of Gamma Cameras with Different Absorber Materials

Ahmed Alharbi

Department of Physics, Qassim University, Qassim 51452, Kingdom of Saudi Arabia
qu.c@hotmail.com

Abstract: Nuclear medicine has a significant role in medical imaging applications which utilizes a certain radioisotope to diagnose different types of diseases. The most common device used in clinics among other imaging detectors is a gamma camera (GC). Such a device is used for different diagnosing purposes including a bone scan, investigating the asymmetries of any organ in the body as well as diagnose cardiac and kidneys abnormalities. In this study, different clinical obtained from different gamma cambers were investigated. The obtained result revealed that gamma cameras have different responses due to various parameters including spatial resolution, the collimator resolution, the intrinsic resolution, as well as the distances from the patients. These parameters highly affect the image quality and details. Furthermore, the comparison between the images obtained by gamma cameras with an X-ray scan showed that GC has a better contras resolution than X-ray which can effectively identify the abnormalities in the projected organs. The processes performed in this lab work can be followed by future work in order to determine the abnormality and asymmetries of any organ of the patent body by using a suitable gamma camera either (HRGP) or (LEHS) ones.
[Ahmed Alharbi. **Detection Efficiency of Gamma Cameras with Different Absorber Materials.** *Nat Sci* 2024,22(3):1-9]. ISSN 1545-0740 (print); ISSN 2375-7167(online). http://www.sciencepub.net/nature 01. doi:10.7537/marsnsj220324.01.

Keywords: Gamma-rays ; Shielding materials; Gamma Cameras

1. Introduction

In nuclear medicine, radionuclides sources play a major role in diagnostic procedures and treatment of various diseases. These radioisotopes can provide a significant indication of the abnormalities in the human body at a very early stage of a disease. Thus, this can potentially lead to cure severe diseases such as cancer and tumor by preventing the spread of rapid cell growth. This diagnostic information can be provided as an image of the human body due to the distribution of the medically inhaled or injected Radiopharmaceuticals emitting gamma rays [1]. The diagnostic test can be performed by different imaging devices that can visualize the physical diagnosis of either an organ or of the whole body. Among these diagnostic techniques employed in nuclear medicine, the Gamma Camera (GC) is widely utilized which can perform functional scans of the emitted radiation from a tracer introduced into the patient's body. However, the detection efficiency of the Gamma Camera is influenced by certain parameters including sensitivity, spatial resolution, and contrast. The low count rates and poor contrast resolution can highly reduce the quality of the final displayed image [2]. This lab report aims to test the GC imaging qualities of different images due to the change in sensitivity and spatial resolution at several distances as a result of using different collimators.

2. Theory

2.1 Gamma Camera (GC)

The Gamma Camera employed in nuclear medical imaging to display and analyze images of the patient body acquired by the distribution of radioisotopes emitting gamma rays. Such a device has three major components include Collimator, Scintillation detector, and Photomultiplier Tubes as illustrated in Figure 1[3].

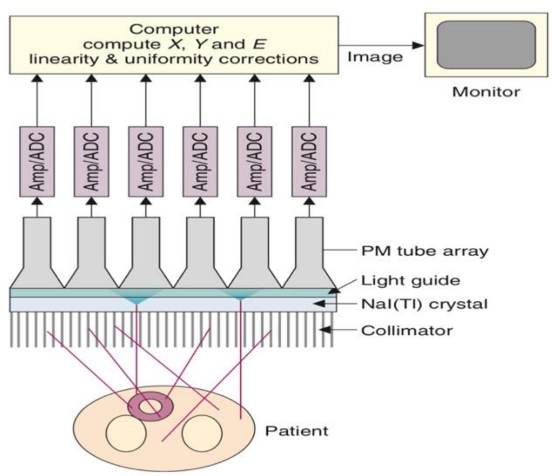

Figure 1. Schematic of gamma camera main components for detecting gamma radiation [2].

The preferred emissions for nuclear medicine application are γ rays in the energy range of 80 to 500 keV (or annihilation photons, 511 keV). A modern GC has an energy resolution of 9% to 10% at 140 keV (^{99m}Tc). However, the details and the quality of an image acquired by GC is influenced by several parameters associated with the image systems. These include spatial and contrast resolution as well as the sensitivity that is determined by the GC components.

2.1.1 Collimator

The collimator is an essential part of any GC, which consists of an array of very tiny holes, usually parallel in a disc of lead material that has a high atomic number and density. This device is the first component of the GC encountering the photon emitted from the radionuclide source and allowing an image of the biodistribution of the gamma ray tracer to be displayed. Thus, it passes only a parallel beam of gamma rays to the scintillator, and any other gamma ray travelling in all other direction will be absorbed in the holes of the collimator as illustrated in Figure 2.

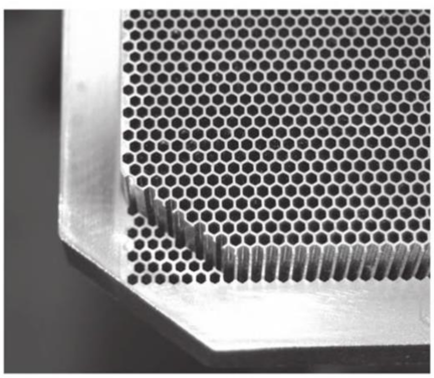

(a)

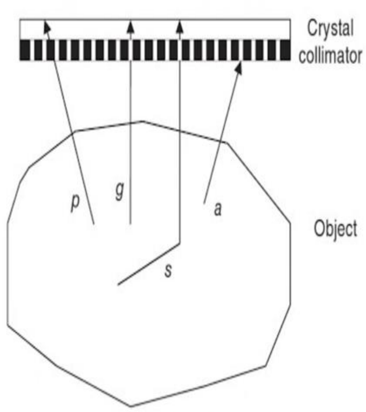

(b)

Figure 2. The construction of the most commonly used parallel-hole collimators with hexagonally shaped (a) and the interaction of the gamma rays with a collimator (b) [4].

In the absence of a collimator in any gamma camera, gamma rays emitted from all different angles are absorbed in the scintillators leading to obtaining very low spatial information. However, with a collimator, only the gamma rays that arrive with a relative angle to the camera that carrying significant information are projected by the scintillation crystal. The other gamma rays that are not coming with proper angle will be absorbed by the lead between the holes (septa).
The collimator, therefore, represents the most significant limitation on the performance of gamma cameras and is the main determinant of the sensitivity and the resolution. These parameters are determined by different factors of the geometric dimensions of the collimator including the distance from the gamma source, the thickness of the septa, and the hole length and diameters. The distance from the object is a prime factor in the collimator resolution. With the increase in the distance from the from the gamma source, the resolution decreased because many gamma rays can pass through a wider area of the collimator without being absorbed in the lead. However, the sensitivity remains approximately as the distance increases because almost the same number of gamma ray pass a large number of holes. This indicates that the optimal collimator requires to be at close distances from the gamma sources [3,4].

2.1.2 The Scintillator and The Photomultiplier (PMT)

The most common type of scintillators used in GC is the NaI(Tl) scintillator compromising an inorganic Sodium Iodide crystal activated by thallium iodide (Tl) connected with a photomultiplier tube (PMT). In the scintillation crystal, the incoming gamma can interact with the electrons of the crystal causing ionization and therefore visible light is emitting. This visible light is converted to electrons in the photocathode of the PMT, amplified by a factor of 10^6, digitized and recorded by an Analog to Digital Converter (ADC). The PMT creates a signal that is proportional to the scintillation light generated in the crystal.

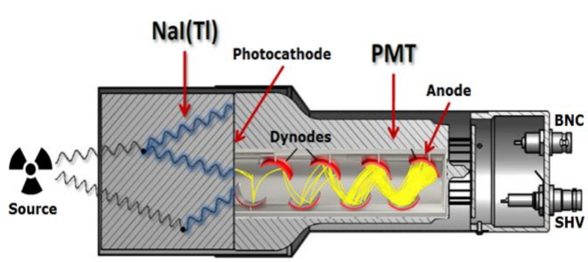

Figure 3. Schematic diagram of the detector with NaI(Tl) crystal and PMT [6].

2.1.3 System Resolution

The quality of images provided by a GC is limited by several factors, including scattered radiation, collimator resolution (R_{coll}), septal penetration, and an intrinsic resolution of the camera (R_{int}). The most important two factors among them are R_{int} and R_{coll} where the combined effect of them produces a system resolution R_{Sys} (FWHM) as given by :

$$R_{sys} = \sqrt{R_{int} + R_{coll}} \qquad (1)$$

The system resolution depends on the distance from the gamma source since the collimator resolution is a function of source-to-collimator distance. The intrinsic resolution of the GC is a measure of the sharpness of the images determined by the combination of the NaI(Tl) scintillator and the PMT[5].

3. Methodology

The experiment started with calculating the sensitivity on a certain region in the image and the count rates of the gamma ray sources of different images. The acquisition time of acquiring the images with the presence of different materials (Latex) and without (air) was 30 seconds. Thus, the obtained count rates of the γ-rays and the sensitivity of each image was plotted as a function of different distances from the collimator. This followed by selecting and displaying various images of normality and abnormalities taken by a gamma camera at different distance and also with different collimators properties. Therefore, comparing the images taken from the same categories to identify any asymmetries between them that indicate an abnormality. The second step was using the appearance of the images at different distances to determine the sensitivity and the intrinsic resolution that are characteristic of the gamma camera used to visualize these images. Furthermore, these clinical images are also utilized for diagnosis purposes of three bone scans and two different kidneys.

4. Experiential Results

4.1. Sensitivity and visual resolution of a gamma camera

The detected count rate of the different images in both air and in Latex (different absorbers) and the sensitivity at various distances from the collimator is shown in Table 1. Therefore, they have been plotted as a function of distance with their corresponding errors as displayed in Figure 4. The sensitivity of the gamma camera has been measured by dividing the count rate at each distance by the source activity which is 74 MBq.

Table1. shows the reduction of the count rate obtained from the images as well as the sensitivity at different distances.

D (cm)	Count rate-Air (cps)	Errors (√count)	sensitivity $=\frac{counts}{74}$ (cps/MBq)	Count rate Latex (cps)	Errors (√count)	sensitivity $=\frac{counts}{74}$ (cps/MBq)
0	342995	±585	4635	342995	±585	4635
8	345073	±587	4663	247154	±497	3339
12.5	344463	±586	4654	201577	±448	2724
24	341599	±584	4616	131913	±363	1782

The results have shown that the count rates of the images are attenuated exponentially as a result of the increase in thicknesses of the different absorbers of the latex. This is due to more scattering This reduction as a function of the absorber's thickness according to the Beer–Lambert's law based on the relationship in the following equation.

$$I = I_0\, e^{-\mu x} \qquad (2)$$

where I_0 is the unattenuated gamma ray intensity (without any absorber), I is the attenuated gamma ray beam intensity after traversing the absorber, μ (cm−1) is the linear attenuation coefficient of the absorber material and x (cm) is the linear thickness.

The half-value thickness of the absorbing material, which represents a 50% reduction in the incoming gamma ray radiation can be determined as follow [4].

$$x_{1/2} = \ln 2/\mu \qquad (3)$$

As shown in Figure 4, the count rate of the gamma ray source is approximately constant with the increase in the distance between the collimator and the source. This is because the gamma ray can traverse a wide range distance without being absorbed or scattered. However, the intensity of gamma ray has reduced exponentially with the presence of the Latex material that leads to more scattering between the radiation and materials.

The linear attenuation coefficient for latex has been obtained from the exponential decay as shown in Figure 4 $\mu = 0.04\ cm^{-1}$, whereas the $I_0 = 339549\ cps$. Therefore, the half thickness for latex material required to decrease the intensities to half of its value can be obtained from equation 3 which equal to $x_{1/2} = \ln 2/\mu = 0.693/0.04 = 17.3\ cm$ for latex.

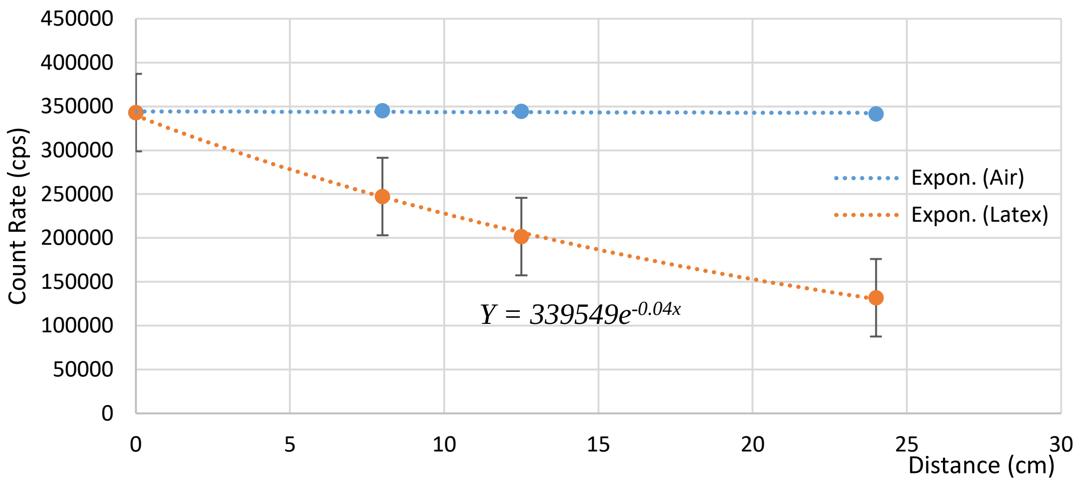

Figure 4. The attenuated gamma rays as a result of Latex materials (orange line), and the approximately constant count rate obtained in air as a function of different distances (blue line).

4.2 Count Rate Response and Resolution of a Gamma Camera

The count rate response of a head in kcts/sec acquired at 30 s from 12 images and their corresponding activity (Bq) value are shown in Table 2. These values of count rate have been plotted versus activity as illustrated in Figure 5.

Table 2. Presents the count number obtained at 30 second and the activity of 12 images with their corresponding error.

Image Number	Activity (Bq)	Count Rate (kcts/s)	Standard deviation of counts (√count)
1	12.2	1.05	1.02
2	51.5	4.16	2.04
3	90.9	7.17	2.67
4	136.6	9.67	3.10
5	379.4	24.58	4.95
6	543.5	33.06	5.75
7	1024	46.36	6.80
8	1429	51.54	7.17
9	2513	42.71	6.53
10	2956	35.37	5.94
11	3331.4	32.02	5.65
12	2091	41.54	6.44

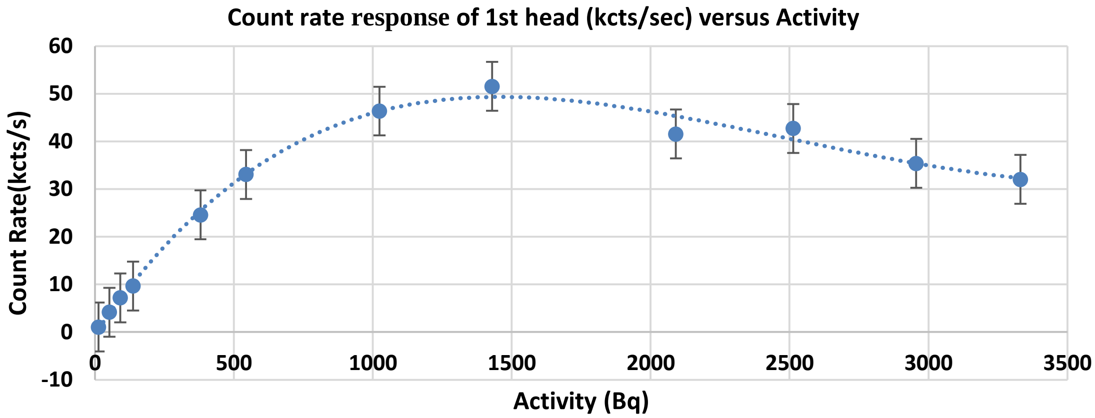

Figure 5. The count rate response of 1st head (kcts/sec) versus Activity (Bq) obtained from 12 images with their error bars.

The count number obtained from each image was divided by 30 seconds to acquire the count rate in kcts/s. As shown in Figure 5 , there was a clear linearity response of the gamma camera until 9.67 (kcts/s). However, at higher count rate than 9.67 (kcts/s), the straight line starts to curve until the gamma camera saturated at high count rate and then the count rates begin to decreases. This saturation of response of the gamma camera at high activities occurred due to the contribution of the Compton scattering gamma ray signals. The Compton scattering of different gamma rays overlaps and combined with each other which therefore detected as a high-count rate pulse. These unwanted scattering events can also affect the uniformity of the image as a result of poor linearity corrections of the detector.

4.2.1 System and Intrinsic Resolution

The quality of images recorded with a GC is limited by several factors, including intrinsic resolution, scattered radiation, collimator resolution (R_{coll}) , septal penetration, and an intrinsic resolution of the camera (R_{int}). The most important two factors among them are R_{int} and R_{coll} where the combined effect of them produces a system resolution R_{Sys} (FWHM) as given by:

$$R_{sys} = \sqrt{R_{int} + R_{coll}}$$ □□□

The system resolution depends on the distance from the gamma source since the collimator resolution is a function of source-to-collimator distance. The intrinsic resolution of the GC is a measure of the uniformity of the images determined by the combination of the NaI(Tl) scintillator and the PMT without a collimator.

The resolution of the collimator represents the sharpness gamma-ray images projected onto the detector. Such resolution is relatively worse than the R_{int} of the gamma camera.

The collimator has different design and types including the high-resolution general purposes (HRGP) and the low-energy high-sensitivity (LEHS). The high-resolution general purposes (HRGP) collimator has a low FWHM value and is typically used for high resolution studies, such as bone scans. The low-energy high-sensitivity (LEHS) collimator is unlike the HRGP which has a high sensitivity rate leading to a poor resolution (High FWHM values) which has a maximum energy of 140keV. The LEHS collimator is specifically suitable for applications that have very low activities such as sentinel lymph nodes in case of melanoma.

The FWHM values of the various images determined by two collimators having different characteristics have been plotted as a function of multiple distances as shown in Figure 6

As displays in Figure 6, the first collimator has a low value of FWHM with the increase of distance indicating that such collimator has high resolution and is a type HRGP. This collimator is highly suitable for bone scans purposes. However, the second collimator has much higher values of the FWHM that proportionally increase with the distances indicating a low-resolution collimator (LEHS). This collimator is primarily utilized in clinical imagining as to identify objects with low activity rate such as the sentinel lymph node [7].

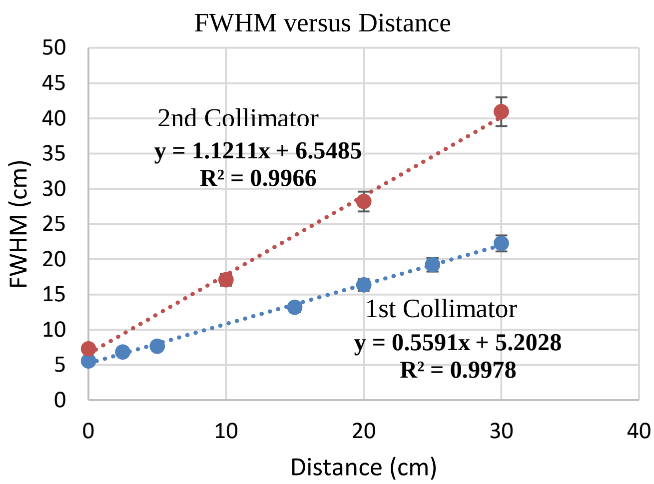

4.3 Bone Scans and Renography

4.3.1 Bone Scans

A bone scan is a nuclear imaging test used for diagnosing purposes to identify an abnormality in the bones that can arise from injury or different diseases. These diseases involving metastatic, primary or secondary bone cancer, fracture, and even minor abnormalities in bone metabolism. In nuclear medicine, bone scan performed by using 99m Technetium methylene diphosphonate (^{99m}Tc MDP) isotopes having activity of 600 MBq and $t_{1/2}=6h$ (140 keV). Therefore, using gamma camera (a scintillation camera) to provide a digitized image of a bone in 3-4 h after injecting the patient with a liquid radionuclide. Bone scans have greater sensitivity as a comparison with x-rays and other modalities for the detection of metastatic bone. This is because bone scan can differentiate between 'shin splints' (periostitis) and stress fractures much better than x-ray, whereas X-ray only used to investigate the size and the shape of the patent bones[6].

4.3.1.1 BONE 12

The image of a slim patient displays ankles, kneecap, as well as shoulder joints and no abnormalities have been observed. However, there are a number of dark regions in some bones which arise from absorption and calcium intake that led to high metabolic activity.

4.3.1.1 BONE_M

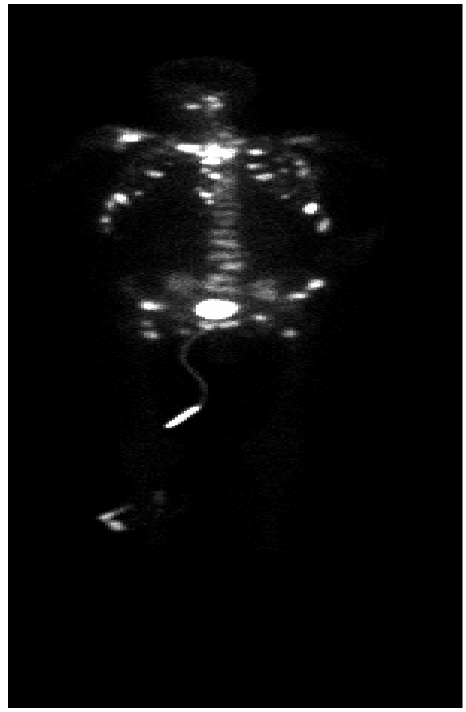

Figure 7. represents a BONE_M image of an abnormal body with an artifact catheter.

As can be seen in the image, there is an artefact catheter appeared on the right knee cap. Similarly, there are several numbers of metastatic disease spread all over the body representing abnormal areas. These diseases can be seen from the region having a high amount of the radioisotope source than others. This includes a bladder and there might be prostate cancer metastasizes in bones and breast cancer. Therefore, the radiotherapy is not applicable for this patient.

4.3.1.3 BONE_B

A digitized image of a normal baby shows some asymmetry in both hands due to fragile bones in baby and inflammation in bones resulting from osteoblastic activity. The right-hand wrist has an abnormal spot due to the build-up of the bones.

4.3.1.4 BONE80

Figure 8. Represents an image of an abnormal fat patient.

The image presents an overweight female with a poor resolution due to a high rate of Compton scattering as the gamma rays traverse more tissues (a fat patient) before reaching the detector. This means that the gamma camera was placed at a high distance from the patient leading to a high reduction in the resolution. There are some asymmetric areas include hip joint and rib, whereas the other parts of the patient body are symmetric. However, better resolution was acquired using an X-ray scan of the same patient with no abnormality. This is because the functional activity is not observed in an X-ray scan opposed to gamma camera that can distinguish abnormalities even with very low resolution.

4.3.2 Kidney scans (Renograms)

The kidney scans are performed to identify and examine the ability of kidneys and their function by using radionuclides. The discharge of the collected radionuclides in the kidneys out of the body represents their ability and any abnormal results that can highlight a misfunction in the kidneys.

4.3.2.1 MAGN-1

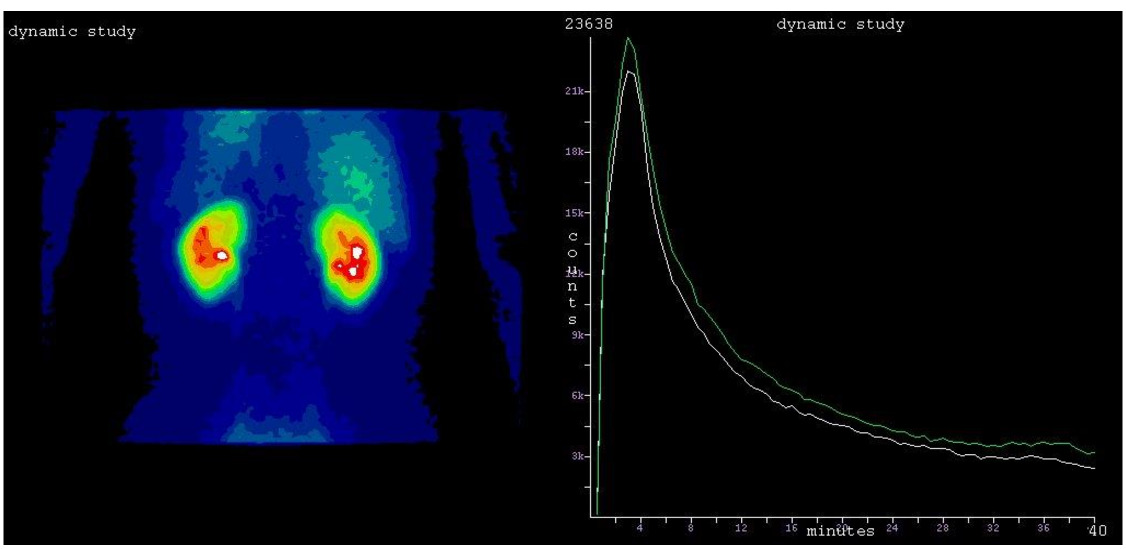

Figure 9. Represents an image of normal kidneys.

4.3.2.2 MAG3O-2

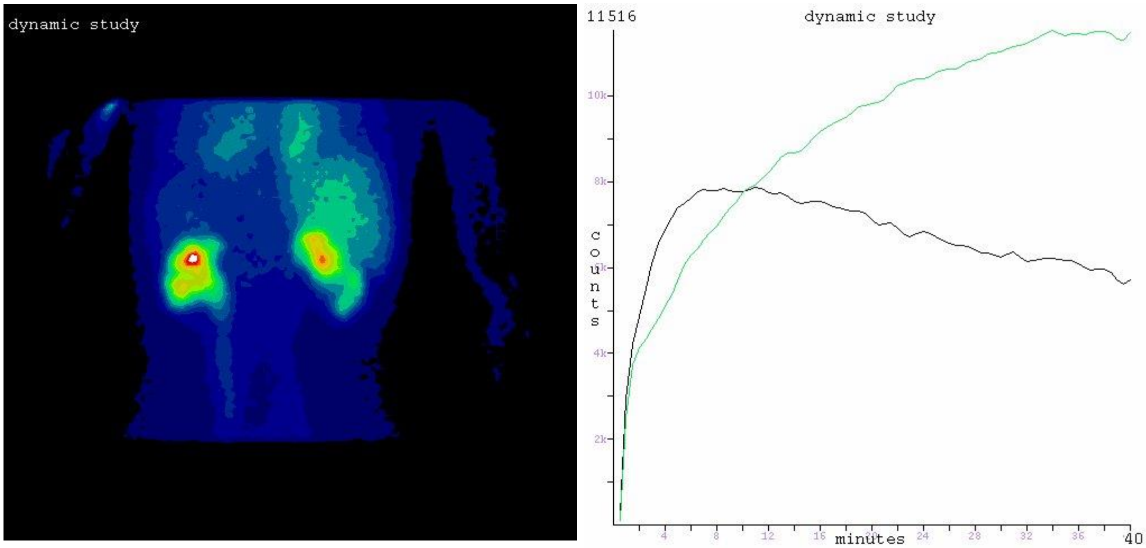

Figure 10. Shows an image of abnormal kidneys.

As can be shown in Figure 9, the activity of the radioactive sours rises in the kidneys until a certain level before being discharged to the bladder and therefore out of the body. There are approximately no differences between the functionality of both kidneys in discharging the radioactive source which means that they are normal.

The image shown in Figure 10, illustrates both kidneys of a patient has abnormality function. As shown in Figure 10, the right kidney has a partial obstruction since the radioactive nuclide liquid slightly discharged to the bladder, whereas the lift kidney indicates approximately full kidney filature. This because the normal kidney can discharge 33000 counts of the radioactive liquid within 12 min while in the case of the right kidney of this patient only a reduction from 8000 counts to 7000 counts of right kidney has been obtained with same period. The left kidney has accumulated significant amount of radionuclide liquids with the increase of time which highly represents a kidney failure [8].

5. Conclusion

The gamma camera is one of the major devices employed in clinics for imaging purposes. Such a device has a different application in nuclear medicine including scanning bones, investigating the asymmetries of any organ in the body as well as diagnose cardiac and kidneys abnormalities which are the most sensitive organs in the body. The common radioisotopes used for diagnosing in clinical imaging is^{99m}Tc which has a very short half-life ($t_{1/2}$= 6h). In this lab work, the obtained result revealed that gamma cameras have different responses due to various parameters including spatial resolution, the collimator resolution, the intrinsic resolution, as well as the distances from the patient. These parameters highly affect the image quality and details. This is primarily due to the effect of different collimators characteristics used in these gamma cameras. Furthermore, the gamma cameras have a better contrast resolution and can identify abnormality greater than X-ray scans that can be only used to show the bone size or shape with no abnormality can be observed. Therefore, for clinical imaging measurement, future work can be built on this lab report by using a suitable gamma camera device either (HRGP) or (LEHS) ones to determine the abnormality of the different diseases that can appear in the patient body.

References

[1] Hine GJ, editor. Instrumentation in nuclear medicine. Academic Press; 2016 Jan 21.

[2] Cherry SR, Sorenson JA, Phelps ME. Physics in nuclear medicine e-Book. Elsevier Health Sciences; 2012 Feb 14.

[3] Bailey DL, Humm JL, Todd-Pokropek A, van Aswegen A. Nuclear Medicine Physics: A Handbook for Teachers and Students. Endorsed by: American Association of Physicists in Medicine (AAPM), Asia–Oceania Federation of Organizations for Medical Physics (AFOMP), Australasian College of Physical Scientists and Engineers in Medicine (ACPSEM), European Federation of Organisations for Medical Physics (EFOMP), Federation of African Medical

Physics Organisations (FAMPO), World Federation of Nuclear Medicine and Biology (WFNMB).

[4] Prekeges J. Nuclear medicine instrumentation. Jones & Bartlett Publishers; 2012 Aug 13.

[5] ELIJAH, K., 2016. *RADIOACTIVITY CONCENTRATIONS AND DOSE ASSESSMENT FOR SOIL SAMPLES FROM WHEAT PLANTATION AREAS OF NAROK COUNTY, KENYA* (Doctoral dissertation, Kenyatta University).

[6] McCroskey WK, Heipp CH, Vickers DS, inventors; SMV America Inc, assignee. Gamma camera for PET and SPECT studies. United States patent US 6,072,177. 2000 Jun 6.

[7] Knoll P, Mirzaei S, Schwenkenbecher K, Barthel T. Performance evaluation of a solid-state detector based handheld gamma camera system. Frontiers in Biomedical Technologies. 2014;1(1).

[8] Hauser W, Atkins HL, Nelson KG, Richards P. Technetium-99m DTPA: a new radiopharmaceutical for brain and kidney scanning. Radiology. 1970 Mar;94(3):679-84.

[9] Sievert H, Qureshi S, Wilson N, Hijazi ZM, editors. Percutaneous interventions for congenital heart disease. CRC Press; 2007 Mar 20.

2/22/2024